



ELSEVIER

Catalysis Today 41 (1998) 229–238

**C**  
TODAY  
CATALYSIS  
TODAY

# Surface sites of microcrystals: Coordination and reactivity

Salvatore Coluccia\*, Leonardo Marchese

*Dipartimento di Chimica IFM, Via P. Gluria, 7-10125 Torino, Italy*

## Abstract

Studies on powders are of great interest in all fields of materials science. For fundamental research, it is relevant to determine the structure of solids at the “boundary” with the external environment where relaxation, reconstruction, adsorption and related phenomena occur. In the case of technological research, application for catalysis, pigments, etc., detailed information are required on morphology of the particles, surface structure, optical properties, adsorptive capacities and so on. The relations between structure and activity of surface sites of typical microcrystalline samples are here focused giving particular emphasis to the role of the coordination of the active centres. © 1998 Elsevier Science B.V. All rights reserved.

**Keywords:** Surface sites; Oxides; Modelling; Infrared; HRTEM

## 1. Introduction

Highly dispersed systems show large specific surface area, typically in the range of  $10\text{--}500\text{ m}^2\text{ g}^{-1}$ . A very important consequence is that a large proportion of atoms or ions are located at the surface of micro-particles, so that the surface itself largely determines characteristics and properties of powders.

Powders are highly disordered, irregular, rough and heterogeneous solids, so that the determination of their structure, and specifically, the surface texture is not straightforward and very rarely results are unambiguous. Relevant contributions come from the studies of reference systems such as model single crystals, which are simpler solids and allow the adoption of very sophisticated and sensitive techniques [1]. However, properties of powders may be significantly different from those of massive samples, so that the interest for

direct studies is maintained both in fundamental and applied research.

Dealing with catalysts, an ultimate goal is determining nature and structure of active sites and reaction mechanisms. Properties of surface sites depend on a number of parameters, obviously correlated, such as dispersion, nature of support, morphology of particles, oxidation state and coordination. The last one is always relevant, influencing the electron distribution (acid–base character) and the tendency to produce surface species.

Numerous physical and chemical techniques are available for catalysts characterization such as:

1. classic optical spectroscopies (UV–vis absorption and emission, IR and Raman) which evidence both intrinsic surface states and adsorbed species;
2. high resolution electron microscopy (HRTEM) showing the exposed faces and microstructures (terraces, steps, edges, etc.), and
3. molecular graphics providing powerful models for detailed description of the solids [2].

\*Corresponding author. Tel.: +3911 6707535; fax: +3911 6707855; e-mail: coluccia@silver.ch.unito.it

More recently, calculations based both on solid state [3] and molecular approaches [4] contribute to the definition of the role of the surrounding structure in determining the overall adsorptive and catalytic activity of sites.

In this report, the potentiality of this strategy is illustrated summarizing typical results obtained with relatively “simple” powders, which can be considered as models because microparticles tend to show much the same morphology and one specific face can be assumed to be dominant.

## 2. Simple oxides

Alkaline earth oxide's catalysts are very convenient systems for surface characterization studies because they can easily be prepared by thermal decomposition of the parent hydroxides or carbonates as finely divided powders ( $200\text{--}10\text{ m}^2\text{ g}^{-1}$ ) which can be treated in vacuo at high temperature without significant loss in specific surface area [5,6]. They are generally regarded as useful models because of their simple rock-salt cubic structure and because the microcrystals predominantly show cube (0 0 1) faces (the contribution of other exposed surfaces can be neglected). Clean surfaces of MgO, CaO, SrO and BaO are produced by outgassing at  $850^\circ\text{C}$ , as even the most resistant surface contaminants like hydroxyl and carbonate groups are desorbed at this temperature [5].

Surface characterization of these oxides was extensively performed by a number of techniques often leading to contrasting hypotheses on the nature of the sites which are involved in adsorption processes and in absorption and emission of light [5–13].

Parallel studies on all alkaline earth oxides showed that powdered samples exhibit absorptions at lower energy than large single crystals and such bands were assigned [5,14] to surface states associated with intrinsic cations and anions exposed in low coordination onto the surface of the oxides, such as  $\text{Mg}_{\text{LC}}^{2+}\text{O}_{\text{LC}}^{2-}$  couples in the case of magnesium oxide. Specifically, three bands were observed in the UV–vis reflectance spectrum of each oxide [14]. Moreover, alkaline earth oxides are photoluminescent and it was found [15] that the excitation spectra show an identical number of bands and in the same position as the bands in the

reflectance spectra. By analogue with bulk excitons, the excitation processes described for powders may be assimilated to the production of excitons which are localized on the surface [14].

These bands are produced by the excitation of 5-coordinated ( $\text{O}_{5\text{C}}^{2-}$ ), 4-coordinated ( $\text{O}_{4\text{C}}^{2-}$ ) and 3-coordinated ( $\text{O}_{3\text{C}}^{2-}$ ) ions exposed on (0 0 1) cube facelets, edges and on corners, respectively. The Madelung constant decreases together with the coordination of the ions and the excitation energy decreases accordingly [14]. Mobility of such excitons can also be evaluated [14]. Such conclusions are supported by theoretical work on a  $\text{Mg}_{21}\text{O}_{20}^{2+}$  cluster showing band gaps for the 3-, 4- and 5-coordinated sites in qualitative agreement with the spectra [16].

Combined spectroscopic and HRTEM studies of magnesium oxide powders provided detailed information on this subject, because MgO can be easily produced in two forms differing considerably in the morphology of the microparticles: (a) MgO-h, prepared by decomposition of the parent hydroxide and (b) MgO-s, prepared by burning magnesium in air [17]. The relative populations of the three families of surface sites with different coordination are significantly different and the reason is immediately evident by inspecting the micrographs in Fig. 1. Details of the rough, highly irregular surface of the particles present in the oxide obtained by thermal decomposition of the hydroxide are illustrated in the high magnification photograph of Fig. 1(A), showing steep successions of steps and small terraces. Consequently, edges and corners are abundant and characteristic features of MgO-h microcrystals.

By contrast, the microcrystals of the smoke (MgO-s) show a nicely shaped cubic habit with edge length in the 45–70 nm range (Fig. 1(B)). Such smoothness is maintained down to the level of a few angstrom, and consequently, the proportion of sites on edges and corners as compared with sites on (0 0 1) planes is much lower. This means that the sites in the lowest coordination (the 3-coordinated sites on the corners and the 4-coordinated sites on the edges) must be comparatively much more abundant in the case of the rough MgO-h than in the case of MgO-s, where 5-coordinated sites on the smooth (0 0 1) microplanes should dominate. As expected, luminescence spectra show that the band due to the most uncoordinated sites (3C, on corners) is relatively more intense for MgO-h

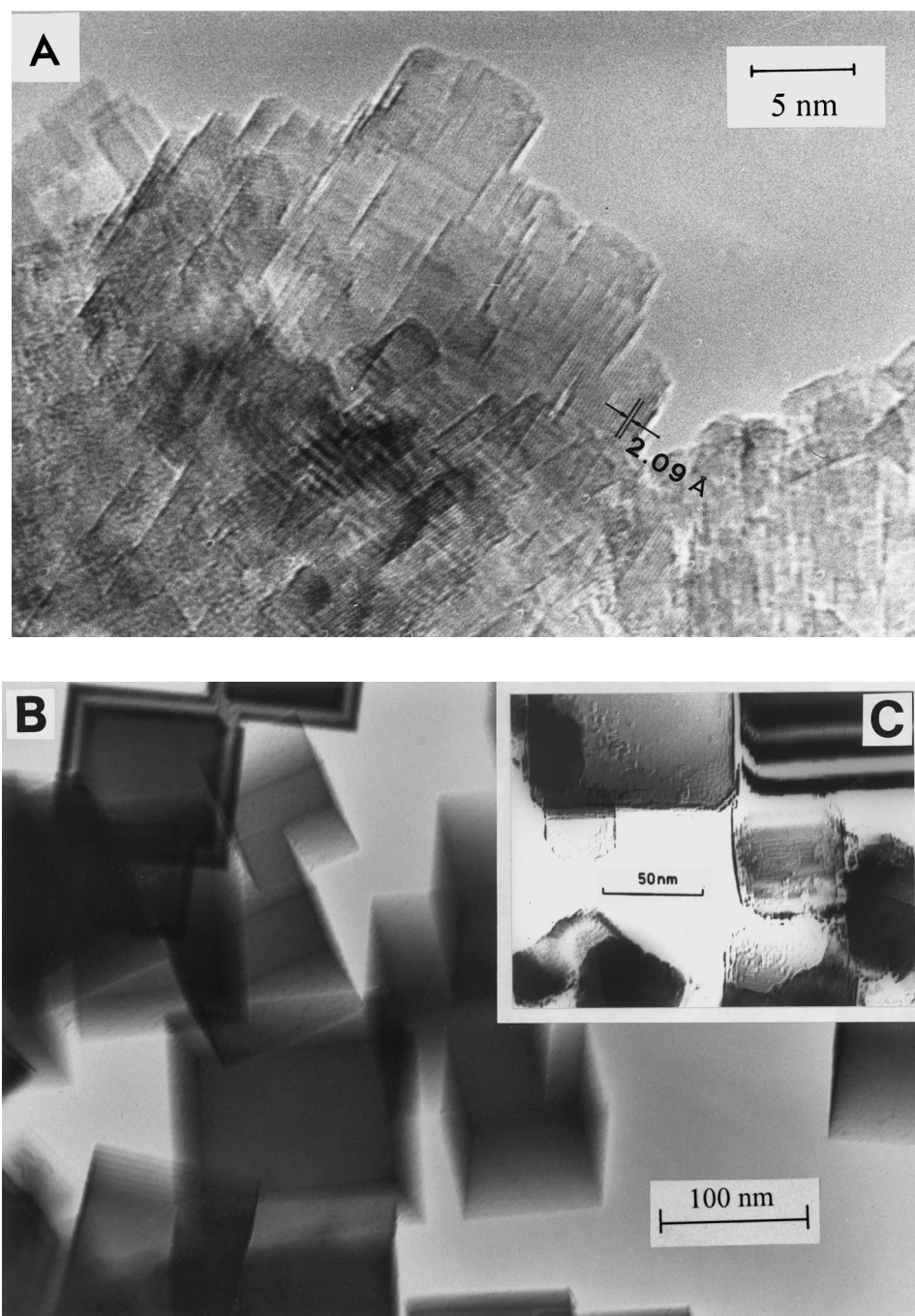


Fig. 1. Various forms of MgO: MgO-ex hydroxide (A), MgO-smoke, as prepared (B) and MgO-smoke eroded by water vapour (C).

than for MgO-s [17]. Most significantly, when the highly perfect shape of the microcubes in the smoke sample is ruined by water attack (Fig. 1(C)), the

population of sites in the lowest coordination increases and the relative intensities of the luminescence bands are heavily affected [17].

## 2.1. Acid sites on simple oxides

It is the dual nature of acid–base couples exposed onto the surface which explains very peculiar aspects of the reactivity of these oxides: heterolytic dissociation of hydrogen containing molecules by breaking H–H, C–H, N–H bonds [18]; production of organic anions and electron transfer processes among adsorbed species [9]; hydrogenation of butadiene [19,20]; isomerization of butenes [21]; oxidative coupling of methane [22]; and CO polymerization [23].

Concentrating our interest, for the moment, on the positive counterpart of the active centres, it is possible to obtain an extensive mapping of the cations by studying the adsorption of carbon monoxide at low temperature. The acid strength of these cations can be monitored by the high frequency shift they induce in the stretching mode of the adsorbed molecule.

Several components appear in Fig. 2(A) (top curve), which shows the spectrum of CO adsorbed on MgO-h at 77 K under a pressure of 10 Torr. Desorption experiments (Fig. 2(A), lower curves) evidence that the various bands are associated with as many surface species with different stability [24] and also allow the identification of further components

which were shadowed by the overwhelming intensity of the main peak in the top curve. CO stretching frequencies higher than that of the free molecule ( $2143\text{ cm}^{-1}$  in the gas phase), are typical of molecules adsorbed on positively charged sites with the carbon pointing towards the cation, the shift increasing as the positive field increases ([24] and references therein). In this case, only cations are present, but different coordinations generate different polarizing power.

Accordingly, the very weak band at the highest frequency ( $2203\text{ cm}^{-1}$ ) has been assigned to CO adsorbed monoxide on  $\text{Mg}_{3\text{C}}^{2+}$  corner sites. Carbon monoxide on  $\text{Mg}_{4\text{C}}^{2+}$  and  $\text{Mg}_{5\text{C}}^{2+}$  are expected to absorb at progressively lower frequencies and the two main bands at  $2159$  and  $2152\text{ cm}^{-1}$ , respectively, are associated with these species [24]. Notice that the extinction coefficients do not vary significantly in this region [25,26] and therefore the relative intensities assignment.

However, the most convincing support to the above assignment comes from the comparison with the spectrum of CO adsorbed on MgO-s (Fig. 2(B)). The population of 5-coordinated sites on the regular and smooth planes of the cubelets of this sample must be overwhelming, and accordingly, only the

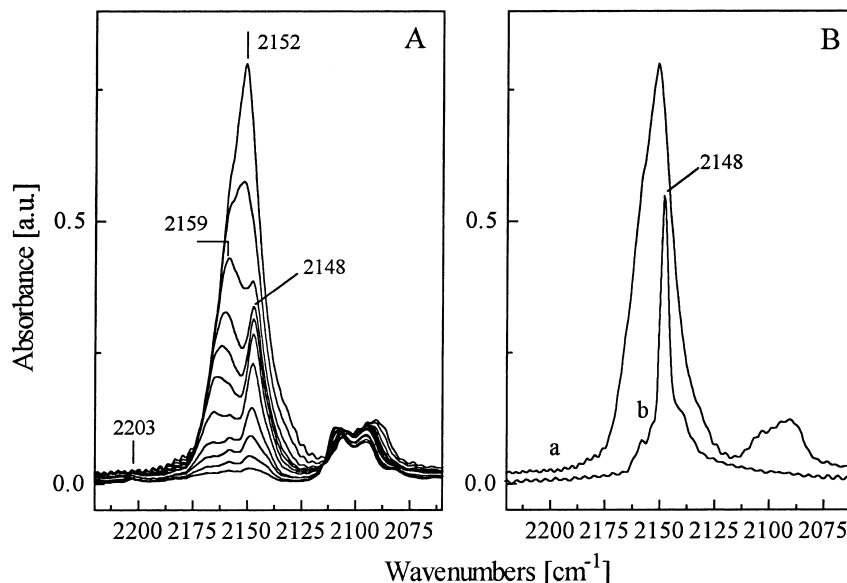


Fig. 2. Section A: IR spectra of CO adsorbed at 77 K on MgO-h under a pressure of 10 Torr (top curve) and under progressively decreasing pressure (lower curves). Section B: Comparison between the spectrum of CO (10 Torr) adsorbed on MgO-h (curve a) and on MgO-s (curve b).

band at lower frequency is observed in curve b of Fig. 2(B).

Other CO bands which are better evidenced at intermediate coverages were believed to be associated with molecules interacting with more than one cation [24]. As such multiple acidic sites might play important roles in adsorption and catalysis, they were also further investigated by other probe molecules.

## 2.2. Multiple acid sites on simple oxides

Multiple sites involving more cations (or anions) on the surface of oxides have been invoked occasionally to interpret specific aspects of reactivity. However, such sites, expected to be very few, have been associated with weak components in the spectra of adsorbed species [24,27–29], and consequently, the attribution of the related infrared bands has often been ambiguous.

Previsions coming from theoretical models have proved to be very helpful in guiding to a detailed assignment of vibrational spectra. Two alternative theoretical approaches are normally adopted for the calculation of adsorption on oxidic catalysts [3,30]:

1. the solid state model, which assumes that, rigorously, a proper description of interactions at the surface requires the infinite solid to be considered [31], either with techniques of infinite solid calculations [32] or quantum mechanical cluster embedded into a set of point charges [33], and
2. the molecular approach based on the assumption that the adsorptive properties of surface sites might be well described by those of a limited number of atoms in molecular models [3,34].

These two standpoints reflect the different expectations on the importance of the long-range contributions to the adsorptive properties of the active sites. An interest for the development of molecular techniques certainly lies in the technological simplicity and much lower computational costs.

The latter approach was assumed to model the adsorption of acetonitrile on the various sites expected to show on the surface of highly dispersed MgO. This molecule has long been used to evidence the acidity of adsorbing centres [35,36], because its CN stretching frequency exhibits a dependence on the strength of the electron-donor interaction via the nitrogen lone pair

with Lewis acids. This is the consequence of the stabilization of the  $\sigma$ -orbital of the CN group following the electron donation from the nitrogen lone pair to the positive centre. Shifts to frequencies higher than that of the free molecule in the vapour phase are produced under these circumstances.

The infrared spectrum of  $\text{CD}_3\text{CN}$  molecularly adsorbed on MgO essentially showed four overlapped bands [37] in the  $2350\text{--}2293\text{ cm}^{-1}$  range, the assignment of which was not straightforward taking into account only the observed shifts to the CN frequency and the reversibility of the related species. A proposal could be made considering the results of calculations of molecular models (see table 1 and Fig. 3).

However, the most important contributions of the calculations were that:

1. no adsorption should take place on 5-coordinated sites;
2. the nitrile could be stabilized by multiple sites consisting of a couple of 4-coordinated cations and a couple of 3-coordinated cations; and
3. no stabilization is expected on more complex sites (triplets of cations).

The calculated shifts for adsorption on multiple sites indicated that two bands at  $2317$  and  $2280\text{ cm}^{-1}$  had to be assigned to molecules interacting with  $2\text{Mg}_{4\text{C}}^{2+}$  and with  $2\text{Mg}_{3\text{C}}^{2+}$  centres as shown in Fig. 3.

## 2.3. Basic sites on simple oxides

Surprisingly enough, it was found that carbon monoxide, the most widely used probe molecule for acid sites, is also a very sensitive “spy” molecule for basicity. In fact, the adsorption of CO at room temperature on MgO was unambiguously attributed to the reactivity of anions in the lowest coordination ( $\text{O}_{3\text{C}}^{2-}$ ) exposed in corner positions onto the surface of microcrystals [38–40].

The spectra obtained upon adsorption of carbon monoxide on MgO-h samples are very complex, and though the assignment of these spectra underwent continuous revisions [38–42], which will certainly continue, some conclusions have been reached on the nature of the adsorbed species and on the mechanisms of formation. Considering the dependence of the various families of bands on: (a) the pressure of CO in contact with the catalysts; (b) desorption treatments; (c) the temperature of adsorption and (d) time of

**Table 1:**  $\Delta\nu(\text{CN})$  shifts of  $\text{CD}_3\text{CN}$  ( $\text{cm}^{-1}$ )

site	model	calc	exp
Mg <sub>3</sub> c	<b>1a</b>	26	30
Mg <sub>4</sub> c	<b>1b</b>	24	21
Mg <sub>5</sub> c	<b>1c</b>	1	-
2-Mg <sub>3</sub> c	<b>2a</b>	4	8
2-Mg <sub>4</sub> c	<b>2b</b>	42	45
3-Mg <sub>3</sub> c	<b>2c</b>	-26	-

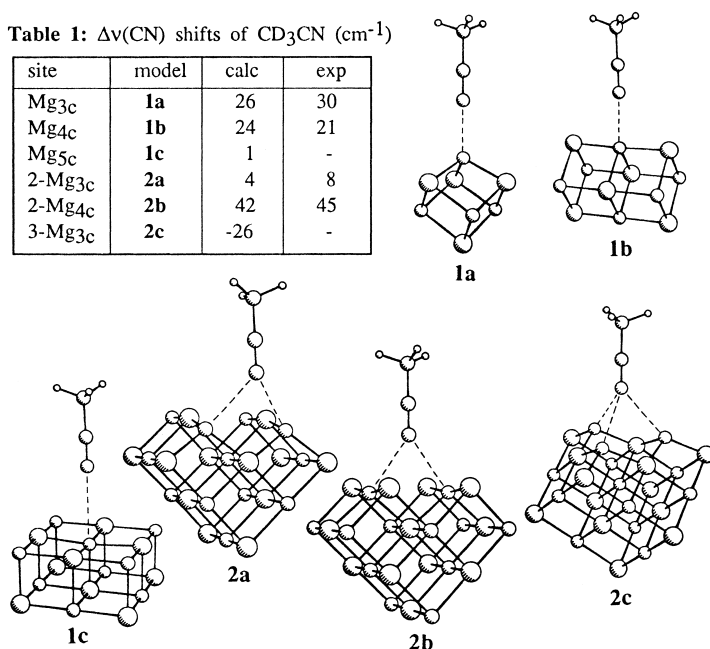


Fig. 3. Molecular models and CN vibrational frequency shifts (Table 1 reports both experimental and calculated values [37]) for the adsorption of  $\text{CD}_3\text{CN}$  on single and multiple  $\text{Mg}^{2+}$  sites.

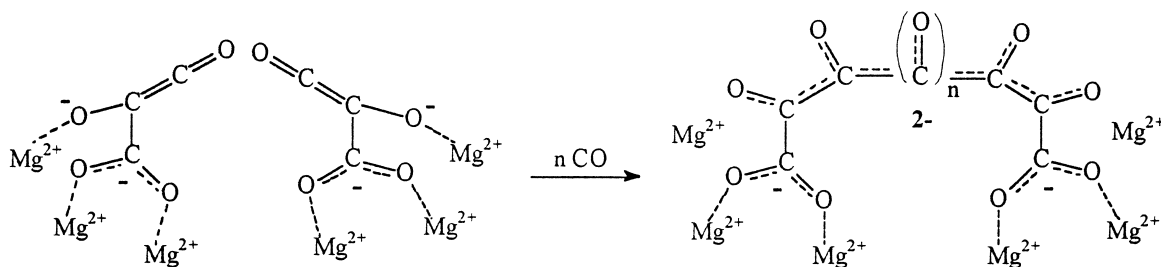
contact, it was proposed that, starting from relatively simple precursors, complex anionic polymers of CO are produced by the following steps:

1. transient  $\text{CO}_2^{2-}$  species, clearly identified by their vibrational bands in the spectra at low temperature [38,41], are precursors for trimeric entities;
2. some trimeric species may add further CO molecules and produce more complex polymers with either cyclic [39], or more likely, linear structures [41] (see Scheme 1);
3. these polymers further evolve with time producing by fragmentation, both oxidized carbonate-like

groups and reduced entities, the structure of which has not yet been identified.

### 3. Complex oxides

Transition aluminas can be accepted as example of more “complex oxides”, as the same cation ( $\text{Al}^{3+}$ ) can be found in different coordination states. In fact, in trigonal  $\alpha\text{-Al}_2\text{O}_3$  all cations are octahedrally coordinated, transition aluminas have spinel structures and  $\text{Al}^{3+}$  cations occupy both octahedral and tetrahedral positions. It has to be also considered that normal



Scheme 1.

spinel contains two types of metal cations, with tetrahedral divalent cations and octahedral trivalent, while in transition aluminas all cations are trivalent and therefore few positions must be left vacant to compensate the overall charge. However, vacancies represent about 10% of cations' sites and can be neglected in this presentation.

This situation is complex in the bulk and may appear even more complex on the surface, where various types of coordinatively unsaturated octahedral and tetrahedral cations should be exposed. Further heterogeneity is produced by the highly irregular morphology of the microparticles in most transition aluminas showing a high number of different faces.

For these reasons, the assignment of the various bands observed in the complex infrared spectrum of CO adsorbed on such surfaces to probe the acidic sites [43] was not considered fully satisfactory [44].

It was important, therefore, to look for a "model" transition  $\text{Al}_2\text{O}_3$  powder, with microcrystals as homogeneous as possible and limited by very few types of faces (ideally, only one). Reller and Cocke [45] found that Alon C Degussa, which can be assumed to be a  $\delta$ - $\text{Al}_2\text{O}_3$ , phase [44,46], answered such requirements as it is constituted by small, flat and nearly hexagonal microcrystals prevalently exposing (1 1 0) faces.

This observation is sustained by the infrared spectrum of adsorbed CO, which shows one major band with maximum at  $2184\text{ cm}^{-1}$  at full coverage and minor components only observable at very low coverages. By contrast, the spectrum of CO adsorbed at the same temperature (77 K) on a standard, morphologically ill defined  $\gamma$ -alumina was more complex [43].

However, it was noticed [44] that the spectrum of CO adsorbed at 77 K was too poor of components even for an "ideal"  $\text{Al}_2\text{O}_3$ , material like Alon C, because cations of two types (octahedral and tetrahedral) are certainly present and should, reasonably, be evidenced by separate bands in the spectra of adsorbed CO as observed with other aluminas. Indeed, the only band observed could be associated with molecules stabilized by ex-tetrahedral  $\text{Al}^{3+}$  exposed, in low coordination, on the surface and no evidence of ex-octahedral cations appeared [43].

A reasonable explanation was proposed considering various possibilities for the (1 1 0) termination of spinel microcrystals with the help of molecular graphics modelling [44].

### 3.1. Possible (1 1 0) surface termination on $\delta$ - $\text{Al}_2\text{O}_3$ powder

A section of a crystal along the [1 1 0] direction is represented in Fig. 4(a), showing that crystal planes containing only octahedrally coordinated cations alternately pile up with planes containing both octahedral and tetrahedral cations. An obvious way of creating surface planes might be cutting the crystal by line 1 shown in Fig. 4(a) and the effect of breaking all bonds encountered is shown in Fig. 4(b) and (c).

Two parts are generated by this procedure, limited by surfaces perpendicular to the [1 1 0] direction and illustrated in Fig. 4(A) and (B). Such surfaces are very much different, because (B) exhibits ex-octahedral cations only, with two coordination vacancies, whereas (A) contains both ex-octahedral with two vacancies, and ex-tetrahedral ones, with one vacancy. It can be noticed that  $\text{O}^{2-}$  anions are equally distributed while cations are not. Termination A has a lower number of cations than B, and consequently, the former carries a negative and the latter a positive charge. Considering the repetitive units [44], it was found that plane A has a  $+1$  charge and plane B a  $-1$  charge. It is generally accepted that charged surface is not stable and would reconstruct. A normal procedure to simulate this process and obtain electrically neutral structures would be to transfer, in rather arbitrary ways, a proper number of  $\text{O}^{2-}$  ions from plane B to A. It can be easily evidenced, however, that this would generate anions and also cations in very low coordination, which would increase the tendency to reconstruct. The overall result is unsatisfactory, as stable surface structures are not obtained. It may be advantageous to cut the crystal so as to obtain, directly, electrically neutral surfaces. Two such ways have been attempted. When the crystal is cut by line 2 shown in Fig. 4(a), two identical terminations are produced as evidenced in Fig. 4(d) and (e). The structure of such surfaces perpendicular to the [1 1 0] direction is illustrated in Fig. 4(c), and the electrical neutrality was verified considering the evidenced repetitive unit [44]. Only ex-octahedral cations are exposed in this case, as tetrahedral ones remain fully coordinated and not accessible. Two different families of ex-octahedral cations are however present, one with two coordination vacancies and the other with three coordination vacancies.

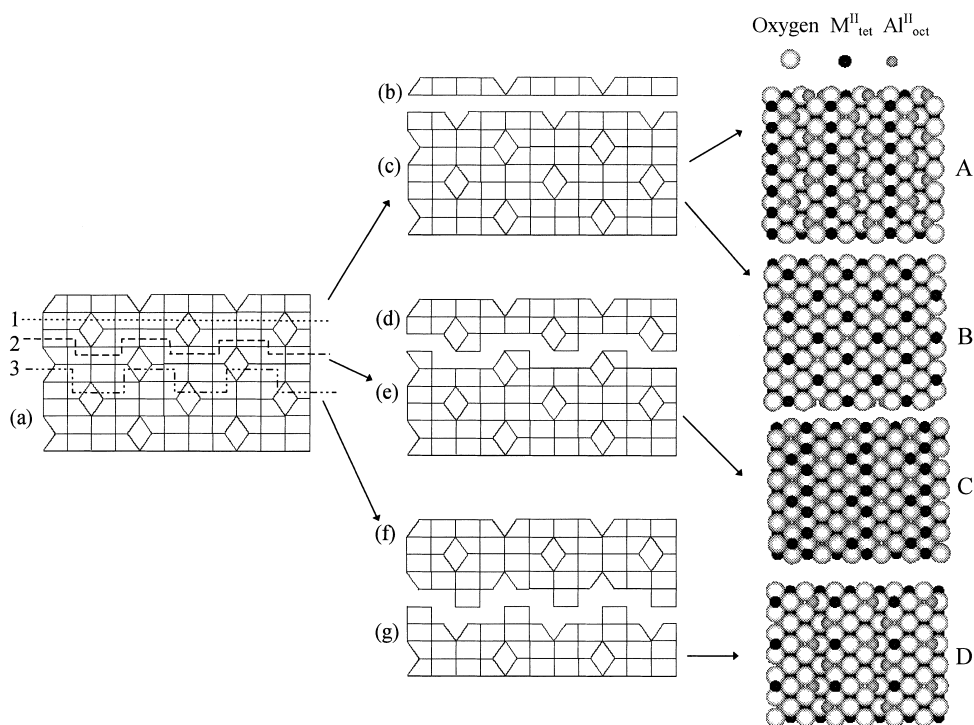


Fig. 4. Computer-generated models of spinel structures representing various terminations for (1 1 0) planes of  $\delta\text{-Al}_2\text{O}_3$ .

By cutting as indicated by the line in Fig. 4(a), both ex-octahedral and ex-tetrahedral cations are exposed and Fig. 4(f) and (g) show that, again, two identical and neutral terminations are generated. The structure of these surfaces is illustrated in Fig. 4(D). It may be noticed that all ex-octahedral cations, this time, exhibit three coordinative vacancies and all ex-tetrahedral only one. The consequence is that all exposed cations are tri-coordinate.

### 3.2. Structure of surface sites on $\delta\text{-Al}_2\text{O}_3$

The above analysis of various possible terminations for the microcrystals of  $\delta\text{-Al}_2\text{O}_3$  has shown that the scheme depicted in Fig. 4(D) might well be a realistic model of the surface structure of an Alon C  $\delta$ -alumina. In fact, all  $\text{Al}^{3+}$ , whatever their original coordination in the bulk, are 3-coordinated when exposed on the surface generated by a proper cut. The situation may justify the fact that one band is dominant in the spectrum of adsorbed CO, because all cations showing the same coordination are expected to exhibit the same polarizing power and to produce the same frequency shift.

The low frequency shift of the band of CO adsorbed on  $\delta\text{-Al}_2\text{O}_3$  Alon C as the coverage increases, was attributed to coupling effects among the vibrating CO molecules in the adsorbed layer [44,47,48]. This was taken as a further evidence of the fact that ordered arrays of similar adsorbed CO molecules are formed, because this is the condition for static and dynamic interactions to occur.

Finally, very weak bands observed at low coverages were assigned to relatively rare sites on corners and edges of the microcrystals [44], also by comparison with similar  $\text{Al}^{3+}$  sites in extremely exposed position in zeolites [49].

## 4. Coordination and mobility of cations in zeolites

Though widely used in industrial catalysis, zeolites are ideal model systems because of the regularity of their porous structure. The presence of  $\text{Al}^{3+}$  in place of  $\text{Si}^{4+}$  in the aluminium–silicate frame produces negative charges which can be balanced, for instance,



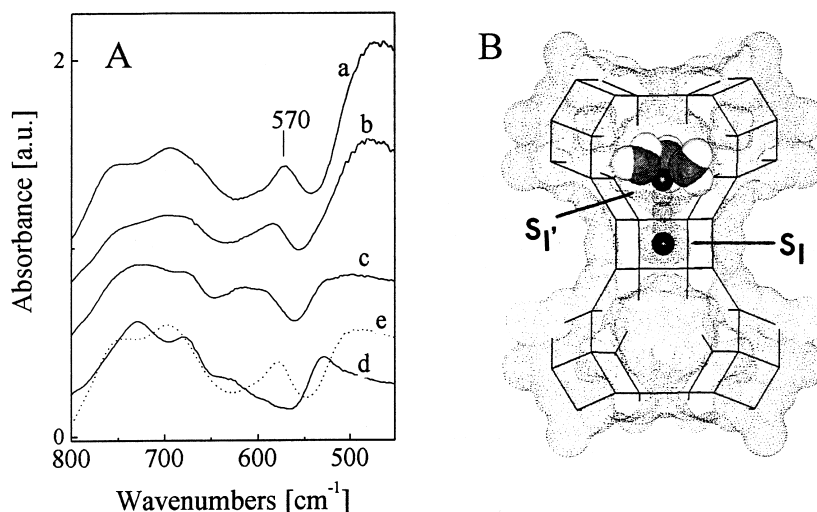


Fig. 5. Section A: IR spectra MgX (section A) outgassed at: (a) 300; (b) 323; (c) 373 and (d) 473 K. Curve (e) is a readsorption of water vapour on the MgX sample and subsequent outgassing at 300 K. Section B: Computer generated model of the motion of a  $\text{Mg}^{2+}$  ion from site I to site I' subsequent to water adsorption (reprinted from [53], Copyright 1995, The Royal Society of Chemistry).

by Brønsted  $\text{H}^+$  ions. The protons may be exchanged by different counter-cations, typically monovalent ( $\text{Na}^+$ ,  $\text{K}^+$ , etc.) or divalent ( $\text{Mg}^{2+}$ ,  $\text{Ca}^{2+}$ , etc.) cations.

The structural characteristics of counter-cations in zeolites have been widely studied with a number of techniques [50–52]. Infrared spectroscopy also is effective in giving information on the overall structure of such solids, and specifically, on location of cations. It has been shown, for example, that pretreatment conditions affect the various cations differently [53].

Fig. 5 shows and compares the spectra of Mg-X zeolites (Linde Molecular Sieves 13X,  $\text{Si}/\text{Al}=1.2$ ) after the outgassing at progressively increasing temperature from 300 to 473 K. The only consequence of this treatment is the elimination of water molecules, “physisorbed” into the cavities, which can be monitored by the disappearance of bands (not reported in the figure) at  $1630\text{ cm}^{-1}$  (H–O–H bending mode) and at  $3000\text{--}3700\text{ cm}^{-1}$  (O–H stretching modes) [53].

The bands in the  $400\text{--}800\text{ cm}^{-1}$  range (Fig. 5(A)) are due to stretching and bending modes involving Al–O and Si–O bonds [51,54], and it is widely accepted that some can be assumed to be specifically associated with vibrations inside tetrahedral units ( $\text{TO}_4$ , where T is either Si or Al), while others involve more units. It was noticed that no significant modifications of the spectra are produced upon dehydration in the case of Na-X (spectra not shown), whereas a

band at  $570\text{ cm}^{-1}$  is heavily affected in the case of Mg-X: it gradually shifts and disappears as water is removed (curves a–d), and most significantly, is fully restored as water is readmitted (curve e). This process can be repeated indefinitely with identical effects [53].

The dependence of the spectrum of Mg-X on the hydration state was interpreted assuming that:

1. in the presence of excess water, the coordination sphere of  $\text{Mg}^{2+}$  ions located in the supercages and in the sodalites contains both  $\text{H}_2\text{O}$  molecules and oxygen atoms of the framework [55];
2. upon outgassing,  $\text{H}_2\text{O}$  ligands are removed, and the divalent cations move to sites where the positive charge can be more efficiently shielded by frame oxygen atoms; and
3. as the  $570\text{ cm}^{-1}$  band is very sensitive to the structural features of the hexagonal prismatic units [54], the spectral changes indicate, in particular, that  $\text{Mg}^{2+}$  located in I' sites may move to I sites where they are octahedrally surrounded by six oxygen lattice atoms, so producing a deformation of the oxygen rings which constitute the windows between prisms and sodalites.

This process is illustrated in section B of Fig. 5[53]. The space available for the movement of the cation was evaluated by the Connolly algorithm [56] using as probe a sphere with the radius of the  $\text{Mg}^{2+}$  ion.

Direct evidence of the transfer of  $\text{Mg}^{2+}$  was also obtained by the spectra in the far infrared region, where the stretching vibrations of the cations against lattice in different sites produce separate bands [53].

## References

- [1] D.W. Goodman, *Chem. Rev.* 95 (1995) 523.
- [2] A. Zecchina, D. Scarano, S. Bordiga, G. Ricchiardi, G. Spoto, F. Geobaldo, *Catal. Today* 27 (1996) 403.
- [3] J. Sauer, P. Ugliengo, E. Garrone, V.R. Saunders, *Chem. Rev.* 94 (1994) 2095.
- [4] J.B. Nicholas, A.C. Hess, *J. Am. Chem. Soc.* 116 (1994) 5428.
- [5] A. Zecchina, M.G. Lofthouse, F.S. Stone, *J. Chem. Soc., Faraday* 1 71 (1975) 1476.
- [6] A. Zecchina, F.S. Stone, *J. Chem. Soc., Faraday* 1 72 (1976) 2364.
- [7] D. Cordischi, V. Indovina, M. Occhiuzzi, *J. Chem. Soc., Faraday Trans.* 1 74 (1978) 883.
- [8] S. Coluccia, A.J. Tench, in: T. Seiyama, K. Tanabe (Eds.), *Proceedings of the Seventh International Congress on Catalysis*, part b, Elsevier, Amsterdam, 1981, p. 1154.
- [9] M. Che, A.J. Tench, *Adv. Catal.* 31 (1982) 77–32 (1983) 1 and references therein.
- [10] V.A. Shvets, A.V. Kuznetsov, V.A. Fenin, V.B. Kazansky, *J. Chem. Soc., Faraday Trans.* 1 81 (1985) 2913.
- [11] M. Anpo, Y. Yamada, *Mater. Chem. Phys.* 18 (1988) 465.
- [12] S. Coluccia, in: M. Schiavello (Ed.), *Photocatalysis and Environment*, Kluwer Academic Press, London, 1988, p. 191.
- [13] S. Coluccia, L. Marchese, in: M. Schiavello (Ed.), *Photocatalysis and Environment*, Kluwer Academic Press, London, 1988, p. 205.
- [14] E. Garrone, A. Zecchina, F.S. Stone, *Phyl. Mag. B* 42 (1980) 683.
- [15] S. Coluccia, A.M. Deane, A.J. Tench, *J. Chem. Soc., Faraday Trans.* 1 74 (1978) 2913.
- [16] S.P. Mehandru, A.B. Anderson, J.F. Brazdil, *J. Chem. Soc.* 110 (1988) 1715.
- [17] S. Coluccia, A.J. Tench, R.L. Segall, *J. Chem. Soc., Faraday Trans.* 1 75 (1979) 1769.
- [18] E. Garrone, A. Zecchina, F.S. Stone, *J. Catal.* 62 (1980) 396.
- [19] Y. Tanaka, Y. Imizu, H. Hattori, K. Tanabe, in: T. Seiyama, K. Tanabe (Eds.), *Proceedings of the Seventh Congress on Catalysis*, part b, Elsevier, Amsterdam, 1981, p. 1254.
- [20] S. Coluccia, L. Marchese, in: K. Tanabe, H. Hattori, T. Yamaguchi, T. Tanake (Eds.), *Acid–Base Catalysis*, Kodansha, Tokyo, 1989, p. 207.
- [21] M. Anpo, Y. Yamada, S. Coluccia, A. Zecchina, M. Che, *J. Chem. Soc., Faraday Trans.* 1 85 (1989) 609.
- [22] R.H. Nibbelke, J. Scheerova, M.H.J.M. de Croon, G.B. Marin, *J. Catal.* 156 (1995) 106.
- [23] A. Zecchina, F.S. Stone, *J. Chem. Soc. Chem. Commun.* (1974) 582.
- [24] S. Coluccia, M. Baricco, L. Marchese, G. Martra, A. Zecchina, *Spectrochim. Acta* 49A (1993) 1289.
- [25] D.A. Seanor, C.H. Amberg, *J. Chem. Phys.* 42 (1965) 2967.
- [26] V. Bolis, B. Fubini, C. Morterra, *J. Chem. Soc., Faraday Trans.* 1 85 (1989) 1383.
- [27] S. Coluccia, F. Boccuzzi, G. Ghiotti, C. Morterra, *J. Chem. Soc., Faraday Trans.* 1 78 (1982) 2111.
- [28] E. Knozinger, K.H. Jacob, P. Hofmann, *J. Chem. Soc., Faraday Trans.* 89(7) (1993) 1101.
- [29] M. Bensitel, O. Saur, J.C. Lavalley, *Mater. Chem. Phys.* 28 (1991) 309.
- [30] G.M. Zhidomirov, V.B. Kazansky, *Adv. Catal.* 34 (1986) 131.
- [31] E.A. Colbourn, *Surf. Sci. Rep.* 15 (1993) 281.
- [32] E.H. Teunissen, C. Roetti, C. Pisani, A.J.M. de Man, A.P.J. Jansen, R. Orlando, R.A. Van Santen, R. Dovesi, *Modell. Simul. Mater. Sci. Eng.* 2 (1994) 921.
- [33] G. Pacchioni, T. Minerva, P.S. Bagus, *Surf. Sci.* 275 (1992) 450.
- [34] A.G. Pelmenschikov, G. Morosi, A. Gamba, S. Coluccia, *J. Phys. Chem.* 99 (1995) 15018.
- [35] V.N. Filimonov, D.S. Bistrov, *Opt. Spectrosc.* 12 (1962) 31.
- [36] K.F. Purcell, *J. Chem. Phys.* 89 (1967) 6139.
- [37] A.G. Pelmenschikov, G. Morosi, A. Gamba, S. Coluccia, G. Martra, E.A. Pankshits, *J. Phys. Chem.* 100 (1996) 861.
- [38] L. Marchese, G. Marta, S. Coluccia, in: R.C.A. Catlow, A.K. Cheetham (Eds.), *New Trends in Materials Chemistry*, NATO ASI Series, vol. 498, Kluwer Academic Press, 1997, p. 79.
- [39] E. Guglielminotti, S. Coluccia, E. Garrone, L. Cerruti, A. Zecchina, *J. Chem. Soc., Faraday Trans.* 1 75 (1979) 96.
- [40] M.A. Babaeva, D.S. Bystrov, A.Yu. Kovalgin, A.A. Tsygankenko, *J. Catal.* 123 (1990) 396.
- [41] A. Zecchina, S. Coluccia, G. Spoto, D. Scarano, L. Marchese, *J. Chem. Soc., Faraday Trans.* 86 (1990) 703.
- [42] L. Marchese, S. Coluccia, G. Martra, E. Giamello, A. Zecchina, *Mater. Chem. Phys.* 29 (1991) 237.
- [43] A. Zecchina, E.E. Platero, C.O. Areàn, *J. Catal.* 107 (1987) 244.
- [44] L. Marchese, S. Bordiga, S. Coluccia, G. Martra, A. Zecchina, *J. Chem. Soc., Faraday Trans.* 89 (1993) 3483.
- [45] A. Reller, D.L. Cocke, *Catal. Lett.* 2 (1989) 91.
- [46] G. Busca, P.F. Rossi, V. Lorenzelli, M. Benaissa, J. Travert, J.C. Lavalley, *J. Phys. Chem.* 89 (1989) 433.
- [47] P. Hollins, J. Pritchard, *Surf. Sci.* 89 (1979) 486.
- [48] R. Disselkamp, H.C. Chanc, G.E. Ewing, *Surf. Sci.* 240 (1990) 193.
- [49] L.M. Kustov, V.B. Kazansky, S. Beran, L. Kubelkova, P. Jiru, *J. Phys. Chem.* 91 (1987) 5247.
- [50] C. Brémard, M. Le Maire, *J. Phys. Chem.* 97 (1993) 9695.
- [51] W.P.J.H. Jacobs, J.H.M.C. van Wolput, R.A. van Santen, *Zeolites* 13 (1993) 170.
- [52] G.A. Ozin, M.D. Baker, J. Godber, W. Shihua, *J. Am. Chem. Soc.* 107 (1985) 1995.
- [53] G. Martra, N. Damianno, S. Coluccia, H. Tsuji, H. Hattori, *J. Chem. Soc., Faraday Trans.* 91 (1995) 2961.
- [54] E.M. Flanigen, in: J.A. Rabo (Ed.), *Zeolite Chemistry and Catalysis*, ACS Monograph, vol. 171, ch. 2, American Chemical Society, Washington, DC, 1976, p. 80.
- [55] A.A. Anderson, Y.F. Shepelev, Y.I. Smolin, *Zeolites* 10 (1990) 32.
- [56] M.L. Connolly, *J. Appl. Crystallogr.* 16 (1983) 548.